Experimental Dermatology ADF

House Dust Mite-Treated PAR2 Over-Expressor Mouse; A Novel Model of Atopic Dermatitis.

Journal:	*Experimental Dermatology*
Manuscript ID	EXD-19-0165.R1
Manuscript Type:	Regular Article
Date Submitted by the Author:	n/a
Complete List of Authors:	Smith, Leila; University College Dublin, Charles Institute of Dermatology Gatault, Solene; University College Dublin, Charles Institute of Dermatology Casals-Diaz, Laura; Almirall Prodesfarma Centro de Investigación y Desarrollo, Skin Biology and Pharmacology Kelly, Pamela; University College Dublin, Department of Veterinary Pathology Camerer, Eric; Paris Centre of Cardiovascular Research, INSERM U970 Metais, Charles; University College Dublin, Charles Institute of Dermatology Knaus, Ulla; University College Dublin, Conway Institute, School of Medicine Eissner, Günther; University College Dublin, Systems Biology Ireland Steinhoff, Martin; Hamad Medical Corporation, Department of Dermatology; University College Dublin, Charles Institute of Dermatology
Area of Expertise:	Atopic dermatitis
Keywords:	ATOPIC DERMATITIS, SKIN BARRIER, INFLAMMATION
Additional Keywords:	Atopic dermatitis, mouse model, protease-activated receptor 2, house dust mite, skin barrier

TITLE

House Dust Mite-Treated PAR2 Over-Expressor Mouse; A Novel Model of Atopic Dermatitis.

AUTHORS

Leila Smith, BA,[1] Solène Gatault, PhD,[1] Laura Casals-Diaz, PhD,[2] Pamela A. Kelly, FRCPath, MRCVS,[3] Eric Camerer, PhD,[4] Charles Métais, PhD,[1] Ulla G. Knaus, PhD,[5] Günther Eissner, PhD,[6] and Martin Steinhoff, MD, PhD[1,7]

[1]Charles Institute of Dermatology, School of Medicine, University College Dublin, Dublin 4, Ireland; [2]Skin Biology and Pharmacology, Almirall R&D Centre, Sant Feliu de Llobregat, Barcelona, Spain; [3]Department of Veterinary Pathology, School of Veterinary Medicine, University College Dublin, Dublin 4, Ireland; [4]INSERM U970, Paris Cardiovascular Research Centre, Paris, France; [5]Conway Institute, School of Medicine, University College Dublin, Dublin 4, Ireland; [6]Systems Biology Ireland, University College Dublin, Dublin 4, Ireland; [7]Department of Dermatology, Hamad Medical Corporation and Qatar University, Doha, Qatar.

CONFLICTS OF INTEREST

L. Casals-Diaz is an employee of Almirall, S.A.

CORRESPONDING AUTHOR

Ms. Leila Smith, Charles Institute of Dermatology, School of Medicine, University College Dublin, Belfield, Dublin 4, Ireland. Phone: +353-1-716-6347. Email: leila.smith@ucdconnect.ie.

KEY WORDS

Atopic Dermatitis, mouse model, protease-activated receptor 2, house dust mite, skin barrier.

ABSTRACT

Background: Atopic Dermatitis (AD) is a complex skin disease involving causative effects from both intrinsic and extrinsic sources. Murine models of the disease often fall short in one of these components and as a result, do not fully encapsulate these disease mechanisms.

Objective: We aimed to determine whether the protease-activated receptor 2 over-expressor mouse (PAR2OE) with topical house dust mite (HDM) application is a more comprehensive and clinically representative AD model.

Methods: Following HDM extract application to PAR2OE mice and controls, AD clinical scoring, itching behaviour, skin morphology and structure, barrier function, immune cell infiltration and inflammatory markers were assessed. Skin morphology was analysed using haematoxylin and eosin staining and barrier function was assessed by transepidermal water loss measurements. Immune infiltrate was characterised by histological and immunofluorescence staining. Finally, an assessment of AD-related gene expression was performed using quantitative RT-PCR.

Results: PAR2OE mice treated with HDM displays all the characteristic clinical symptoms including erythema, dryness and oedema, skin morphology, itch and inflammation typically seen in AD patients. There is a significant influx of mast cells ($p<0.01$) and eosinophils ($p<0.0001$) into the dermis of these mice. Furthermore, the PAR2OE + HDM mice exhibit similar expression patterns of key differentially expressed genes as seen in human AD.

Conclusion: The PAR2OE + HDM mouse presents with a classic AD pathophysiology and is a valuable model in terms of reproducibility and overall disease representation to study the condition and potential therapeutic approaches.

ABBREVIATIONS

AD: Atopic dermatitis

BCA: Bicinchoninic acid assay

CXCL1: Chemokine (C-X-C motif) ligand 1

DAPI: 4',6-diamidino-2-phenylindole

FLG: Filaggrin

GAPDH: Glyceraldehyde 3-phosphate dehydrogenase

GZMB: Granzyme B

HDM: House dust mite

IEL: Intraepithelial lymphocyte

IL-4: Interleukin-4

IL-36γ: Interleukin-36 (gamma isoform)

IVL: Involucrin

LOR: Loricrin

MADAD: Meta-analysis-derived atopic dermatitis

MPO: Myeloperoxidase

PAR2: Protease-activated receptor 2

PAR2OE: Grhl3$^{PAR2/+}$ over-expressor mouse

RIPA: Radioimmunoprecipitation assay buffer

RT-qPCR: Real-time quantitative polymerase chain reaction

SDS: Sodium dodecyl sulfate

TEWL: Trans-epidermal water loss

Th_1: T helper Type 1 cell

Th_2: T helper Type 2 cell

Th_{17}: T helper Type 17 cell

T_{reg}: Regulatory T cell

WT: Wild-type mouse

INTRODUCTION

Atopic Dermatitis (AD) is a common, chronic inflammatory and pruritic skin disease [1]. It affects up to 25% of children worldwide, the majority of whom present with symptoms within the first year of life, however up to 70% of patients will go into remission in adolescence [2,3]. Patients present with erythematous, pruritic papules predominantly on the inner folds of skin. As the disease progresses from an acute to a chronic stage, lesions become lichenified as a result of persistent damage due to inflammation and scratching. The etiology of AD is not fully understood, however, two classical mechanistic hypotheses exist that attempt to explain the complex mechanisms present within the disease. The first, known as the "Inside-Out" hypothesis suggests that AD results from inherently high levels of Th_2 cytokines within the skin that drive inflammation and skin barrier disruption [4]. Release of cytokines such as IL-31; an itch-mediator, can provoke barrier damage through scratching [5]. Other mediators that target keratinocytes include IL-6 which can inhibit essential ceramide synthesis and IL-22 that downregulates gene expression of cornified cell envelope genes, e.g. filaggrin and cathepsin d [6,7]. The second hypothesis, known as the "Outside-In" hypothesis suggests that AD results from fixed, genetic barrier defects (such as filaggrin null-mutation) that allow entry to the skin by allergens and pathogens [4]. This causes inflammation which results in further barrier breakdown through the mechanisms outlined above. While the literature supports either of these pathways, ultimately it appears that AD may occur as a result of both disease mechanisms operating concurrently.

Unfortunately, many murine models do not accurately reflect this prevailing theory and are generated through use of one or other of the classical mechanistic hypotheses. Cytokine-overexpressing mice such as the IL-4tg and IL-31tg mice exhibit AD-like dermatitis and inflammation. However, the inflammation is restricted to a Th_2 response which is not typical of AD as it has been well-documented that T cell subsets in AD vary between Th_2, Th_{17}, Th_1

and T_{reg} depending on the disease stage [8]. Murine models such as the transgenic *Flg*-mutant (*Flg*$^{ft/ft}$) or the spontaneous flaky-tail (*Tmem*79$^{ma/ma}$ *Flg*$^{ft/ft}$) mouse have genetic barrier disruption through loss-of-function filaggrin mutations. However, this model is not translatable as not all patients with AD have skin barrier mutations nor does the presence of such a mutation always result in disease [9]. Application of haptens such as oxazolone are commonly used to generate acute AD models through repeated exposure while single exposure is more often used as a model of allergic contact dermatitis [10]. The overlap here presents a debateable assertion in distinguishing between the two forms of skin inflammation and whether the resulting phenotype is in fact AD. Finally, one of the best-characterised AD murine models; the NC/Nga mouse with house dust mite (HDM) application, also falls short due to its application of topical sodium dodecyl sulfate (SDS) to the skin prior to HDM application [11]. SDS application to murine skin is a well-known inducer of irritant contact dermatitis and again, causes difficulty in establishing the precise nature of the dermatitis seen in the model.

Protease-activated receptor 2 (PAR2) is a G-protein-coupled receptor that has been linked to multiple aspects of dermatitis including skin barrier function, inflammation and itch [12-15]. It is activated via proteolytic cleavage of its extracellular N-terminus, which in turn acts as the specific ligand for the receptor. It had previously been shown that over-expression of the PAR2-activating enzyme cathepsin S in mice could induce AD-like symptoms, suggesting a key role for this receptor in the disease [16]. Initial generation of a mouse with PAR2 over-expression in the epidermis revealed dermatitis-like symptoms including epidermal hyperplasia, ichthyosis and itch [17]. HDM is frequently used in the generation of AD murine models and it contains many allergenic trypsin-like proteases that may cleave and activate the PAR2 receptor [18,19]. Furthermore, many AD patients have high IgE levels specific to HDM allergens and avoidance of HDM can lead to improvement of clinical symptoms in patients

[20,21]. In order to develop an improved AD model, we sought to combine both the inherent PAR2 over-expression and associated barrier dysfunction with exposure to HDM and resulting allergic inflammation. We hypothesised that the presence of both disease mechanisms would better represent the human disease phenotype and accelerate the development of the dermatitis present in PAR2 mice. We found that the mice presented with a reproducible, clinical dermatitis consistent with human AD in aspects such as morphology, immunology and skin barrier function.

METHODS

Animals

Heterozygous Grhl3$^{PAR2/+}$ (PAR2OE) and FvB/n wild type (WT) mice were housed in 12hr light/dark cycle in individually ventilated cages. Routine monitoring and testing verified that mice were free from infectious pathogens. Mice were genotyped by PCR using genomic DNA from ear-punch biopsies. Primers used are listed in Supplementary Table 1. Eight-week old mice were shaved on the neck and back on day -1. The following day, 100mg of HDM ointment (Biostir, Inc., Osaka, Japan) was applied to the neck and ears of mice and thereafter twice/week for a total of six weeks. All experiments were reviewed and approved by the University College Dublin Animal Research Ethics Committee and the Health Products Regulatory Agency of Ireland.

Clinical Assessment

Weight and clinical score were evaluated at each HDM application. A cumulative clinical score out of 12 was calculated from individual values for the symptoms of erythema, oedema, erosion and dryness of the skin (absent (0), mild (1), moderate (2) or severe (3)). Following the final HDM-application, scratching was assessed over multiple 10 minute intervals by double-blind video recording as previously described [22]. A single scratching bout was defined as the period between which a mouse raised its hindpaw to its body and subsequently lowered it or began grooming. Transepidermal water loss (TEWL) and ear thickness measurements were taken using an AS-WT100RS VapoScan (Asahi Biomed Co., Kanagawa, Japan) and an electronic caliper respectively.

Histological Staining

Ear skin was fixed in 4% (w/v) paraformaldehyde overnight and embedded in paraffin wax. Standard hematoxylin and eosin staining was performed on 5µm sections using an autostainer (Leica Biosystems, Nussloch, Germany). For Giemsa staining, sections were deparaffinized and rehydrated followed by 45 minute incubation in Giemsa stain (Sigma Aldrich, Saint Louis, MO). Sections were rinsed with distilled water and fixed with ethanol. Alkaline Sirius Red stain was prepared according to Llewellyn et. al [23]. After rehydration, sections were incubated in Mayer's hematoxylin for 8 minutes followed by 30 second destaining with acid alcohol. Sections were then incubated in alkaline Sirius Red for 2 hours followed by tap water rinse to remove excess stain. Epidermal thickness and quantification of infiltrating immune cells was performed in 3-6 fields of view at 200X magnification in a blinded fashion using ImageJ software (National Institutes of Health, Bethseda, MD). Care was taken to select fields within the dermis that did not include large blood vessels, glands, muscle or cartilage. Human punch biopsy skin samples were acquired with informed consent and in accordance with the Ethics and Medical Research Committee, St. Vincent's University Hospital, Dublin 4, Ireland.

Immunofluorescence and Immunohistochemical Staining

Deparaffinized and rehydrated sections were subjected to heat-induced antigen retrieval in sodium citrate buffer (pH6.0). Sections were blocked with donkey serum prior to incubation with either anti-mouse CD3 (1:500, Abcam, Cambridge, United Kingdom), anti-mouse Ly6G (1:250, Biolegend, San Diego, CA), or normal rabbit IgG control (1:250, R&D Systems, Minneapolis, MN) overnight at 4°C. Post-incubation with anti-rabbit Alexa Fluor®568 conjugated antibody (1:1000, Invitrogen, Carlsbad, CA) or anti-rat Alexa Fluor®488 conjugated antibody (1:1000, Cell Signalling Technologies, Danvers, MA) for 2 hours at

room temperature, sections were counterstained with DAPI. Images at X200 and X400 were taken using an IX83 Fluorescent Inverted Microscope (Olympus, Tokyo, Japan).

ELISA Analysis

Tissue was snap frozen and mechanically homogenised in RIPA buffer with protease inhibitors using a TissueLyser LT (Qiagen, Hilden, Germany). Proteins were extracted and quantified using the Pierce BCA protein assay kit (Thermo Fisher, Waltham, MA). Myeloperoxidase (MPO) was measured in samples using a DuoSet ELISA kit (R&D Systems) following the manufacturer's instructions.

RNA Isolation and Quantitative RT-PCR

Total RNA was extracted and purified from ear tissue using a Nucleospin® RNA Isolation kit (Macherey-Nagel, Düren, Germany) and quantified with a Nanodrop 2000 (Thermo Fisher). Complementary DNA was synthesised from 0.5ug of total RNA with a reverse transcription kit (Thermo Fisher). Quantitative RT-PCR was performed using the QuantStudio 7 Flex system (Applied Biosystems, Foster City, MA). Primers for *Il-4*, *Cxcl1*, *Il-36γ*, *Gzmb*, *Cd4*, *Cd8*, *Flg*, *Ivl*, *Lor* and *Gapdh* were purchased from Applied Biosystems and are listed in Supplementary Table 2. The relative change in gene expression was calculated using the ΔΔCt method.

Statistical Analysis

Significance for all experiments excluding fold-change analysis for RT-qPCR, was based on one-way or two-way ANOVA with multiple comparison using Bonferroni correction. RT-qPCR data was analysed using a Student t test. *p<0.05, **p<0.01, ***p<0.001, ****p<0.0001, ns = not-significant.

RESULTS

Heterogenous development of dermatitis in PAR2OE mice.

To better understand the nature and progression of the dermatitis described by Frateschi et. al., we assessed the development of the innate skin inflammation that appears in PAR2OE mice over time in the FvB/n strain background [17]. Clinical symptoms similar to those seen in AD patients started to appear in the PAR2OE mouse around eight weeks of age (Fig. 1A. a-f). At this age, a slight increase in erythema and oedema was observed at the base of the ears which progressed gradually in subsequent weeks towards the tip. By fourteen weeks of age, the entire ear was visibly dry and inflamed and in some mice began to display small abrasions due to intense scratching. From birth, PAR2OE pups were clearly distinguishable from their WT counterparts by their flaky and inflamed tails (Fig. 1B. a-f). Some mice exhibited autoamputation and necrosis in the tail tip or severe swelling, however this did not appear to negatively affect the welfare or behaviour of the mice. The tails continued to present these features as the mice aged and necrotic tips fell off with no further necrosis appearing (Fig. 1B. a-f). Length, girth and bluntness varied greatly between the tails of PAR2OE mice. Dermatitis lesions on the dorsal skin of PAR2OE mice did not appear until ten weeks of age at the earliest (Fig. 1C. a-d). Though not all PAR2OE mice develop such lesions, in those that did, lesion development varied significantly. Some lesions have the appearance of individual, crusty and raised nodules (Fig. 1C. d) while others consist of flat, discoloured areas of dorsal skin (Fig. 1C. b). Overall, the development of skin inflammation in PAR2OE mice is considerably heterogenous between mice.

Clinical and macroscopic features of PAR2OE + HDM mice indicate an AD phenotype.

Groups of WT, WT + HDM, PAR2OE and PAR2OE + HDM mice were assessed based on their clinical and phenotypic characteristics of AD (Fig. 2A. a-d). No clinical AD symptoms were recorded in WT mice though intermittently, mild erythema was seen in the WT + HDM group. Both PAR2OE and PAR2OE + HDM mice had visibly inflamed ears. No erosion was observed in PAR2OE mice during the study, however some PAR2OE + HDM mice displayed abrasions on their ears and necks due to scratching (Fig. 2A. d). After six weeks of topical HDM application to PAR2OE mice, clinical symptoms increased at a significantly higher rate than those of the untreated PAR2OE mice (Fig. 2B. a). Progression of symptoms was homogenous between mice within the PAR2OE + HDM group. Increase in erythema and oedema in the ears of PAR2OE + HDM mice was first seen after 2-3 weeks of HDM application. Dry skin also appeared in the neck area and base of the ears where the HDM was applied. Erosion appeared later to a varying degree in some, but not all PAR2OE + HDM mice as a result of persistent ear scratching.

To determine whether the model presented with increased pruritus, scratching behaviour was monitored in WT, PAR2OE and PAR2OE + HDM mice over multiple 10 minute intervals. Both PAR2OE and PAR2OE + HDM mice exhibited significantly increased numbers of scratching bouts than WT mice; in which no scratching bouts were observed (Fig. 2B. b). No significant difference was seen between the PAR2OE and the PAR2OE + HDM groups in terms of pruritus. No increase in thickness at any location along the ear was seen in WT + HDM mice in comparison to WT mice (Fig. 2B. c). Ear thickness measurements indicated that swelling was greatest in both PAR2OE and PAR2OE + HDM at the base of the ear with lesser degrees of inflammation seen around the tip. There was significantly increased swelling in the middle and base of the PAR2OE + HDM ears in comparison to all other groups. Measurement of TEWL from the neck showed that a significant increase in water

loss occurs only at the site of HDM application in PAR2OE + HDM mice (Fig. 2B. d). There was no significant difference in TEWL between any groups when untreated skin along the back of the mouse was examined. Clinically, the PAR2OE + HDM mouse exhibits a typical AD phenotype and presents with key disease features including pruritus and TEWL.

Histological assessment of PAR2OE + HDM mice displays classical AD morphology.

Hematoxylin and eosin staining of WT and WT + HDM ear sections displayed identical morphological and cellular sub-structure in these control groups (Fig. 3A. a,b). All four layers of the skin (stratum corneum, epidermis, dermis, hypodermis) were visible with minor dermal infiltration. A marked increase in the thickness of the stratum corneum and underlying epidermal layers was seen in both the PAR2OE and PAR2OE + HDM mice (Fig. 3A. c,d). Retention of keratinocyte nuclei in the stratum corneum, parakeratosis, was visible in both PAR2OE and PAR2OE + HDM skin (Fig. 3A. c,d - black arrowheads). The formation of rete ridges (protrusion of epidermis into the dermis) was also evident in PAR2OE + HDM skin (Fig. 3A. d - red arrowheads). Quantification of epidermal thickness revealed that both PAR2OE and PAR2OE + HDM skin have significantly increased thickness (approximately 5-7 times thicker) relative to that seen in WT mice (Fig. 3B. a). These measurements also demonstrate that application of HDM to WT mice did not induce any epidermal thickening. Finally, PAR2OE + HDM mice had significantly higher numbers of dermally-infiltrating cells in comparison with all other groups indicating a higher level of inflammation (Fig. 3B. b). These morphological changes and features of the skin are all characteristic of human AD (Fig. 3C).

PAR2OE + HDM mice have high numbers of innate immune cells that are relevant to AD pathophysiology.

Giemsa staining of ear skin revealed the presence of mast cells in the dermis of PAR2OE + HDM mice (Fig. 4A. a - red arrows). Mast cells were identified by metachromatic staining of granules and round nuclei. Several cells containing bi-lobed nuclei, indicative of eosinophils, were also visible using this stain (Fig. 4A. a - black arrows). Alkaline Sirius red staining of eosinophil granules confirmed high numbers of eosinophils present in the dermis of the PAR2OE + HDM mice (Fig. 4A. b - black arrows). This stain has been shown to provide excellent contrast and specificity as a murine eosinophil stain [24]. The ear skin of PAR2OE + HDM mice showed low numbers of Ly6g+ neutrophils in these mice (Fig. 4B. a-c). At higher magnification, clear staining of Ly6G+ cells adjacent to a dermal blood vessel was evident in a PAR2OE + HDM treated mouse (Fig. 4B. d-e). Negative control staining confirmed the specificity of the Ly6G antibody (Fig. 4B. f). Low numbers of Ly6G+ cells were observed in PAR2OE mice while Ly6G+ cells were absent from the skin of WT and WT + HDM mice (data not shown). Quantification of mast cells following Giemsa staining indicated no significant difference between WT, WT + HDM and PAR2OE groups while the PAR2OE + HDM group were the only mice with significantly increased numbers of mast cells in comparison with WT mice (Fig. 4C. a). Quantification of eosinophils using alkaline Sirius red staining also revealed significant increase in cell numbers in PAR2OE + HDM in comparison with other groups (Fig. 4C. b). MPO concentration in ear lysates confirmed the relatively low abundance of neutrophils across all groups of mice (Fig. 4C. c). Morphological pathology assessment indicates chronic, active mastocytic and eosinophilic perivascular dermatitis with epidermal hyperplasia in the PAR2OE + HDM group consistent with human AD.

Intraepithelial lymphocytes are present in the PAR2OE + HDM mouse model along with key differential gene expression patterns seen in human AD.

High numbers of CD3+ intraepithelial lymphocytes (IELs) were visible in the epidermis of PAR2OE + HDM mice (Fig. 5A. a-c). Further investigation into the classes of T lymphocytes present in the PAR2OE + HDM model indicated no significant upregulation of *Cd8* gene expression, though it did appear to be increased in comparison with other groups (Fig. 5B. a). Interestingly, expression of granzyme B (*Gzmb*); a protease commonly found in CD8+ T cells, was significantly increased in the PAR2OE + HDM group when compared with WT mice (Fig. 5B. b). Expression of the *Cd4* gene was increased significantly in the PAR2OE + HDM mice along with the key Th_2 and AD-relevant cytokine *Il-4* in comparison with WT mice (Fig. 5B. c,d). Additionally, expression of the AD-relevant cytokine *Il-36γ* was significantly and homogenously upregulated in both PAR2OE and PAR2OE + HDM mice when compared to WT mice as was the AD-relevant chemokine *Cxcl1* (Fig. 5B. e,f). Expression of three skin barrier genes (involucrin, loricrin and filaggrin) were assessed in the WT and PAR2OE + HDM groups. While there was no change in expression levels of involucrin, loricrin was significantly downregulated and filaggrin upregulated in comparison with WT controls (Supplementary Fig. 1).

DISCUSSION

The generation of a murine model that accurately represents a human disease, becomes particularly challenging when the disease is a result of complex interactions between multiple immune pathways, skin barrier destruction and neuroimmune communication [25]. In the case of AD, Ewald *et al.* recently compared a selection of commonly used murine models to determine which, if any, best represented the AD phenotype. The authors concluded that all models represented some, but not all aspects of the disease in terms of cytokine networks and epidermal pathology [26]. The models fell clearly into two groups; those with inflammation-driven induction (IL-23 injection, oxazolone, ovalbumin) and those with barrier dysfunction-driven induction (filaggrin-null and flaky tail). Here we present a novel model with both allergic inflammation- (HDM) and barrier dysfunction- (PAR2OE) induced AD that fills the gap left by current models.

The application of HDM is essential for the full and consistent representation of AD in this mouse model. While the PAR2OE mouse alone exhibits dermatitis and lesion formation, this is somewhat variable between mice in terms of time of appearance and manifestation. Lesions on PAR2OE mice following HDM application are more consistent in appearance between mice. In addition, mice display accelerated symptomatic onset just one week post-HDM application. The minimal variation in clinical scoring shows the reproducibility and homogeneity of the model. Furthermore, HDM application is essential for significant increase in TEWL as it is seen only in the neck skin of PAR2OE mice where the HDM was applied and not in untreated, dorsal skin. The consistency seen in the model may also be partly due to the lack of an initial barrier-disrupting event e.g. tape-stripping or SDS application such as in the case of the NC/Nga model [11]. This severe initial trigger has the ability to effect and dictate the progression of the disease in each mouse individually.

Both PAR2OE and PAR2OE + HDM mice show similar levels of pruritus, indicating that the increased inflammation, erythema and erosion seen in the PAR2OE + HDM group is not the sole result of excessive scratching and must be due to other pathophysiological factors at play. Histological staining of PAR2OE and PAR2OE + HDM skin showed a striking morphological resemblance to human AD skin with observable features such as epidermal hyperplasia, oedema, parakeratosis and rete ridge formation. Both total ear thickness and epidermal thickness are substantially increased in PAR2OE + HDM mice in comparison to other groups as a result of epidermal hyperplasia, oedema and dermal cell infiltration. A closer examination of perivascular infiltrates shows high numbers of mast cells and eosinophils typical of AD and atopic diseases [27,28]. The numbers of these cells is increased as HDM provides the allergenic irritant that induces hypersensitivity. In the absence of HDM, PAR2OE mice appear to have a pre-disposition to acquiring this hypersensitivity as they too have elevated eosinophil counts. However, HDM application is crucial for a robust allergic reaction to occur. Neutrophil involvement in AD has been an intensively debated topic with suggestions that occasionally high neutrophil numbers are primarily a result of *Staphylococcus* infections rather than a result of the pathophysiology of AD [29,30]. The PAR2OE + HDM model exhibits relatively low numbers of neutrophils in the dermal infiltrate and a corresponding low concentration of the neutrophil-specific enzyme; myeloperoxidase in comparison to other dermatological diseases such as psoriasis, which have distinguishing neutrophilic involvement [31]. As none of the mice acquired any infection of lesions during the course of the study, this is likely the reason that no significant influx of neutrophils was seen in the skin.

HDM has previously been shown to induce a robust T-cell response in AD skin [32]. This PAR2OE + HDM model presents with high numbers of CD3+ T cells in both the epidermis and dermis. This is similar to what is seen in human AD skin, the pathophysiology of which

is comprised of several different classes of T cells [8,33]. Those IELs which are predominantly CD8+ T cells are essential for lesion initiation and formation in AD skin [34]. While there was no significant upregulation of *Cd8* gene expression, high expression levels of the CD8-associated protease GZMB were present in the PAR2OE + HDM mice, possibly indicating a higher cytolytic activity of these cells or production by other GZMB-expressing cell types such as natural killer cells or keratinocytes under stress conditions [35]. Granzyme B is highly expressed in human AD skin and is capable of degrading proteins such as laminin, fibronectin, E-cadherin and ZO-1 which are essential for epidermal barrier function [36,37]. *Cd4* gene expression along with *Il-4* confirmed the presence of CD4+ Th_2 cells in the model. The up-regulation of *Il-4* and *Cxcl1* in the PAR2OE + HDM mice selectively indicates the occurrence of a Th_2 and Th_{17} response in the skin. These cytokines are well-documented mediators involved in the pathophysiology of AD and are considered biomarkers of disease activity [8,38-40]. While neither are found within the collection of differentially expressed genes identified in the MADAD transcriptome, their high expression is often seen in AD patients and the success of Dupilumab, a therapeutic anti-IL-4Rα antibody, confirms a central role of IL-4 in the disease [41]. *Il-36γ* and *Gzmb* are two of the top-25 upregulated genes in human AD with murine orthologs [26,36]. Both these genes exhibit a similar magnitude increase in the PAR2OE + HDM. Furthermore, in comparison with other AD models, the PAR2OE + HDM mice have a more representative expression level of *Il-36γ* to human AD and therefore may constitute an improved model for the study of IL-36γ in atopic dermatitis [26]. Interestingly, while loricrin expression was significantly reduced in the PAR2OE + HDM mice in comparison with WT controls, filaggrin gene expression was conversely upregulated. The idea of compensatory redundancy within critical barrier gene expression has previously been hypothesised and accounts for the unexpected level of functionality in the skin barrier of several knock-out mice strains [42,43]. *Flg* expression has also been shown to be upregulated

post-barrier injury such as tape stripping, thus could be upregulated in this model as a result of increased scratching [44]. Additionally, Ewald *et al*. found that the only murine models of AD with decreased filaggrin expression were those with intentional loss-of-function mutations within the gene. All other models assessed had an increase in expression levels [26].

Overall, we have identified that the PAR2OE + HDM mouse is a robust and reproducible model representative of human AD. It accurately displays all aspects of the disease pathophysiology including allergic inflammation, pruritus, barrier dysfunction and immune cell involvement. Its highly representative phenotype and broad characterisation of the disease may shed light on additional disease mechanisms at play in the human condition. Clinically, this model can provide valuable insight into the complex pathways that occur in AD. Furthermore, its potential to serve as a preclinical model may provide a more comprehensive analysis of overlapping functions of therapeutic targets for this disease.

ACKNOWLEDGEMENTS

The authors would like to thank the staff at the UCD Conway Institute of Biomolecular and Biomedical Research Genomics and Research Pathology Core Facilities. We would also like to express our gratitude to Dr. Mark d'Alton and the UCD Biomedical Facility staff for their help with the *in vivo* study. Finally, thank you to Prof. Brian Kirby and Dr. Ian McDonald for their help in recruiting patients for skin biopsies. This work was supported by Science Foundation Ireland Principal Investigator award 14/IA/2511 to M.S. and G.E. and the French National Research Agency (ANR-15-CE14-0009) to E.C.

AUTHORS CONTRIBUTIONS

L.S., G.E. and M.S. wrote the manuscript. L.S. and all other authors contributed to the experimental data and reviewed the final manuscript.

REFERENCES

1. Weidinger S, Novak N. Atopic dermatitis. *Lancet (London, England).* 2016;387(10023):1109-1122.
2. Garmhausen D, Hagemann T, Bieber T, et al. Characterization of different courses of atopic dermatitis in adolescent and adult patients. *Allergy.* 2013;68(4):498-506.
3. Silverberg JI. Public Health Burden and Epidemiology of Atopic Dermatitis. *Dermatologic clinics.* 2017;35(3):283-289.
4. Leung DY, Guttman-Yassky E. Deciphering the complexities of atopic dermatitis: shifting paradigms in treatment approaches. *The Journal of allergy and clinical immunology.* 2014;134(4):769-779.
5. Sonkoly E, Muller A, Lauerma AI, et al. IL-31: a new link between T cells and pruritus in atopic skin inflammation. *The Journal of allergy and clinical immunology.* 2006;117(2):411-417.
6. Sawada E, Yoshida N, Sugiura A, Imokawa G. Th1 cytokines accentuate but Th2 cytokines attenuate ceramide production in the stratum corneum of human epidermal equivalents: an implication for the disrupted barrier mechanism in atopic dermatitis. *Journal of dermatological science.* 2012;68(1):25-35.
7. Gutowska-Owsiak D, Schaupp AL, Salimi M, Taylor S, Ogg GS. Interleukin-22 downregulates filaggrin expression and affects expression of profilaggrin processing enzymes. *The British journal of dermatology.* 2011;165(3):492-498.
8. Wang AX, Xu Landen N. New insights into T cells and their signature cytokines in atopic dermatitis. *IUBMB Life.* 2015;67(8):601-610.
9. Palmer CN, Irvine AD, Terron-Kwiatkowski A, et al. Common loss-of-function variants of the epidermal barrier protein filaggrin are a major predisposing factor for atopic dermatitis. *Nature genetics.* 2006;38(4):441-446.
10. Man MQ, Hatano Y, Lee SH, et al. Characterization of a hapten-induced, murine model with multiple features of atopic dermatitis: structural, immunologic, and biochemical changes following single versus multiple oxazolone challenges. *The Journal of investigative dermatology.* 2008;128(1):79-86.
11. Yamamoto M, Haruna T, Yasui K, et al. A novel atopic dermatitis model induced by topical application with dermatophagoides farinae extract in NC/Nga mice. *Allergology international : official journal of the Japanese Society of Allergology.* 2007;56(2):139-148.
12. Lee SE, Jeong SK, Lee SH. Protease and protease-activated receptor-2 signaling in the pathogenesis of atopic dermatitis. *Yonsei medical journal.* 2010;51(6):808-822.
13. Sakai T, Hatano Y, Matsuda-Hirose H, et al. Combined Benefits of a PAR2 Inhibitor and Stratum Corneum Acidification for Murine Atopic Dermatitis. *The Journal of investigative dermatology.* 2016;136(2):538-541.
14. Steinhoff M, Neisius U, Ikoma A, et al. Proteinase-activated receptor-2 mediates itch: a novel pathway for pruritus in human skin. *The Journal of neuroscience : the official journal of the Society for Neuroscience.* 2003;23(15):6176-6180.
15. Steinhoff M, Vergnolle N, Young SH, et al. Agonists of proteinase-activated receptor 2 induce inflammation by a neurogenic mechanism. *Nature medicine.* 2000;6(2):151-158.
16. Kim N, Bae KB, Kim MO, et al. Overexpression of cathepsin S induces chronic atopic dermatitis in mice. *The Journal of investigative dermatology.* 2012;132(4):1169-1176.
17. Frateschi S, Camerer E, Crisante G, et al. PAR2 absence completely rescues inflammation and ichthyosis caused by altered CAP1/Prss8 expression in mouse skin. *Nature communications.* 2011;2:161.
18. Lee HJ, Lee NR, Jung M, Kim DH, Choi EH. Atopic March from Atopic Dermatitis to Asthma-Like Lesions in NC/Nga Mice Is Accelerated or Aggravated by Neutralization of Stratum Corneum but Partially Inhibited by Acidification. *The Journal of investigative dermatology.* 2015;135(12):3025-3033.

19. Reithofer M, Jahn-Schmid B. Allergens with Protease Activity from House Dust Mites. *International journal of molecular sciences.* 2017;18(7).
20. Platts-Mills TA, Mitchell EB, Rowntree S, Chapman MD, Wilkins SR. The role of dust mite allergens in atopic dermatitis. *Clinical and experimental dermatology.* 1983;8(3):233-247.
21. Tan BB, Weald D, Strickland I, Friedmann PS. Double-blind controlled trial of effect of housedust-mite allergen avoidance on atopic dermatitis. *Lancet (London, England).* 1996;347(8993):15-18.
22. Shimada SG, LaMotte RH. Behavioral differentiation between itch and pain in mouse. *Pain.* 2008;139(3):681-687.
23. Llewellyn BD. An improved Sirius red method for amyloid. *The Journal of medical laboratory technology.* 1970;27(3):308-309.
24. Meyerholz DK, Griffin MA, Castilow EM, Varga SM. Comparison of histochemical methods for murine eosinophil detection in an RSV vaccine-enhanced inflammation model. *Toxicologic pathology.* 2009;37(2):249-255.
25. Elias PM, Steinhoff M. "Outside-to-inside" (and now back to "outside") pathogenic mechanisms in atopic dermatitis. *The Journal of investigative dermatology.* 2008;128(5):1067-1070.
26. Ewald DA, Noda S, Oliva M, et al. Major differences between human atopic dermatitis and murine models, as determined by using global transcriptomic profiling. *The Journal of allergy and clinical immunology.* 2017;139(2):562-571.
27. Liu FT, Goodarzi H, Chen HY. IgE, mast cells, and eosinophils in atopic dermatitis. *Clinical reviews in allergy & immunology.* 2011;41(3):298-310.
28. Steinhoff M, Buddenkotte J, Lerner EA. Role of mast cells and basophils in pruritus. *Immunological reviews.* 2018;282(1):248-264.
29. Choy DF, Hsu DK, Seshasayee D, et al. Comparative transcriptomic analyses of atopic dermatitis and psoriasis reveal shared neutrophilic inflammation. *The Journal of allergy and clinical immunology.* 2012;130(6):1335-1343.e1335.
30. Dhingra N, Suárez-Fariñas M, Fuentes-Duculan J, et al. Attenuated neutrophil axis in atopic dermatitis compared to psoriasis reflects T_H17 pathway differences between these diseases. *Journal of Allergy and Clinical Immunology.* 2013;132(2):498-501.e493.
31. Schon MP, Broekaert SM, Erpenbeck L. Sexy again: the renaissance of neutrophils in psoriasis. *Experimental dermatology.* 2017;26(4):305-311.
32. Malik K, Ungar B, Garcet S, et al. Dust mite induces multiple polar T cell axes in human skin. *Clinical and experimental allergy : journal of the British Society for Allergy and Clinical Immunology.* 2017;47(12):1648-1660.
33. Hijnen D, Knol EF, Gent YY, et al. CD8(+) T cells in the lesional skin of atopic dermatitis and psoriasis patients are an important source of IFN-gamma, IL-13, IL-17, and IL-22. *The Journal of investigative dermatology.* 2013;133(4):973-979.
34. Hennino A, Vocanson M, Toussaint Y, et al. Skin-infiltrating CD8+ T cells initiate atopic dermatitis lesions. *Journal of immunology (Baltimore, Md : 1950).* 2007;178(9):5571-5577.
35. Hernandez-Pigeon H, Jean C, Charruyer A, et al. Human keratinocytes acquire cellular cytotoxicity under UV-B irradiation. Implication of granzyme B and perforin. *The Journal of biological chemistry.* 2006;281(19):13525-13532.
36. Ewald DA, Malajian D, Krueger JG, et al. Meta-analysis derived atopic dermatitis (MADAD) transcriptome defines a robust AD signature highlighting the involvement of atherosclerosis and lipid metabolism pathways. *BMC medical genomics.* 2015;8:60.
37. Turner CT, Lim D, Granville DJ. Granzyme B in skin inflammation and disease. *Matrix biology : journal of the International Society for Matrix Biology.* 2017.
38. Di Cesare A, Di Meglio P, Nestle FO. A role for Th17 cells in the immunopathogenesis of atopic dermatitis? *The Journal of investigative dermatology.* 2008;128(11):2569-2571.

39. Werfel T, Allam JP, Biedermann T, et al. Cellular and molecular immunologic mechanisms in patients with atopic dermatitis. *The Journal of allergy and clinical immunology.* 2016;138(2):336-349.
40. Mansouri Y, Guttman-Yassky E. Immune Pathways in Atopic Dermatitis, and Definition of Biomarkers through Broad and Targeted Therapeutics. *Journal of clinical medicine.* 2015;4(5):858-873.
41. Blauvelt A, de Bruin-Weller M, Gooderham M, et al. Long-term management of moderate-to-severe atopic dermatitis with dupilumab and concomitant topical corticosteroids (LIBERTY AD CHRONOS): a 1-year, randomised, double-blinded, placebo-controlled, phase 3 trial. *Lancet (London, England).* 2017;389(10086):2287-2303.
42. Kawasaki H, Nagao K, Kubo A, et al. Altered stratum corneum barrier and enhanced percutaneous immune responses in filaggrin-null mice. *The Journal of allergy and clinical immunology.* 2012;129(6):1538-1546.e1536.
43. Koch PJ, de Viragh PA, Scharer E, et al. Lessons from loricrin-deficient mice: compensatory mechanisms maintaining skin barrier function in the absence of a major cornified envelope protein. *The Journal of cell biology.* 2000;151(2):389-400.
44. Lee HJ, Kim TG, Kim SH, et al. Epidermal Barrier Function Is Impaired in Langerhans Cell-Depleted Mice. *The Journal of investigative dermatology.* 2019;139(5):1182-1185.

FIGURE LEGENDS

FIG 1. **Phenotypic appearance of the PAR2OE mouse varies between mice**. **A,** Comparison of WT (a-c) and PAR2OE (d-f) ears at age 4, 8 and 14 weeks. **B,** Variability in length and appearance of PAR2OE tails at 14 weeks (b-f) in comparison with WT tail (a). **C,** Sporadic appearance of inflammation and lesions indicated by purple arrowheads on dorsal skin of 14 week-old PAR2OE mice (b-d) in contrast to WT (a).

FIG 2. **Clinical and macroscopic features of the PAR2OE + HDM model are representative of human AD. A,** Representative appearance of neck and ears of WT (a), WT + HDM (b), PAR2OE (c) and PAR2OE + HDM (d) mice after 6 weeks with or without HDM treatment. **B,** Clinical characteristics of WT and PAR2OE mice with and without application of HDM; clinical score (a), scratching bouts (b), ear thickness (c) and transepidermal water loss (d). Colour coding of the groups is illustrated in (a). N=5 for all groups except scratching bouts where N=3-4.

FIG 3. Histological and morphological features of the PAR2OE + HDM model resemble human AD skin. A, Haematoxylin and eosin staining of WT (a), WT + HDM (b), PAR2OE (c) and PAR2OE + HDM (d) ear sections. Black arrowheads indicate hypergranulosis and parakeratosis in the stratum corneum. Rete ridge protrusion of the epidermis into the dermis is indicated by red arrowheads. Images shown are representative of each group. N=5 for all groups. **B,** Haematoxylin and eosin staining of normal (a), lesional AD (b) and non-lesional AD (c) human skin. **C,** Quantitative assessment of epidermal thickness (a) and numbers of infiltrating immune cells in the dermis (b) in each group. N=5 for all groups.

FIG 4. The PAR2OE + HDM model features a similar innate immune cell phenotype as human AD. A, Ear skin section of PAR2OE + HDM mouse following Giemsa (a) and Sirius red (b) staining. Dermally infiltrating mast cells are indicated by red arrows; eosinophils are

indicated by black arrows. N=5. **B,** Ear skin section of PAR2OE + HDM mouse following immunofluorescence staining for Ly6G (a-e) and control staining (f) Ly6G-positive cells are indicated by yellow arrows. N=3. **C,** Numbers of mast cells (a) and eosinophils (b) were quantified per region of interest (ROI) in 3-6 ROI per mouse. Myeloperoxidase concentration was quantified by ELISA (c) in ear skin extracts of mice. N=5 for all groups.

FIG 5. **T-cell presence and AD-relevant gene expression patterns are seen in the PAR2 + HDM model. A,** Ear skin sections of PAR2OE + HDM mouse following immunofluorescence staining for CD3 (a-c). The broken yellow line denotes the dermal/epidermal boundary. CD3-positive cells are indicated by white arrows. N=3. **B,** Expression of *Cd8* (a), *Gzmb* (b), *Cd4* (c), *Il-4* (d), *Il-36γ* (e) and *Cxcl1* (f) in ear skin extracts of WT and PAR2OE mice with and without HDM treatment. N=5 for all groups.

A

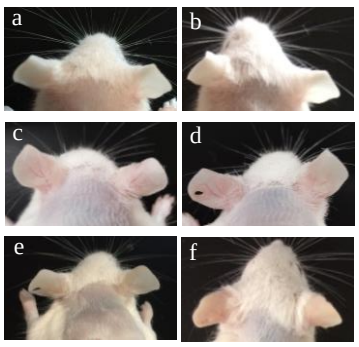
4w
8w
14w
a
b
c
d
e
f
WT Ears
PAR2OE Ears

B

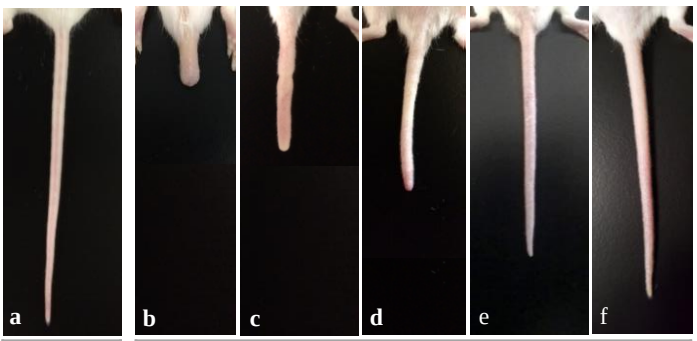
a
b
c
d
e
f
WT Tail
PAR2OE Tails

C

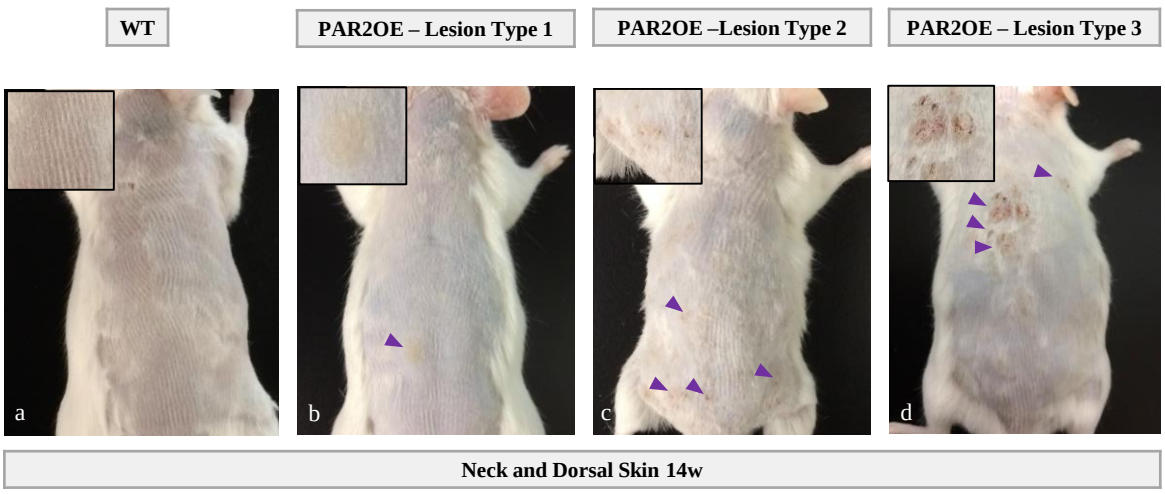
WT
PAR2OE – Lesion Type 1
PAR2OE –Lesion Type 2
PAR2OE – Lesion Type 3
a
b
c
d
Neck and Dorsal Skin 14w

A

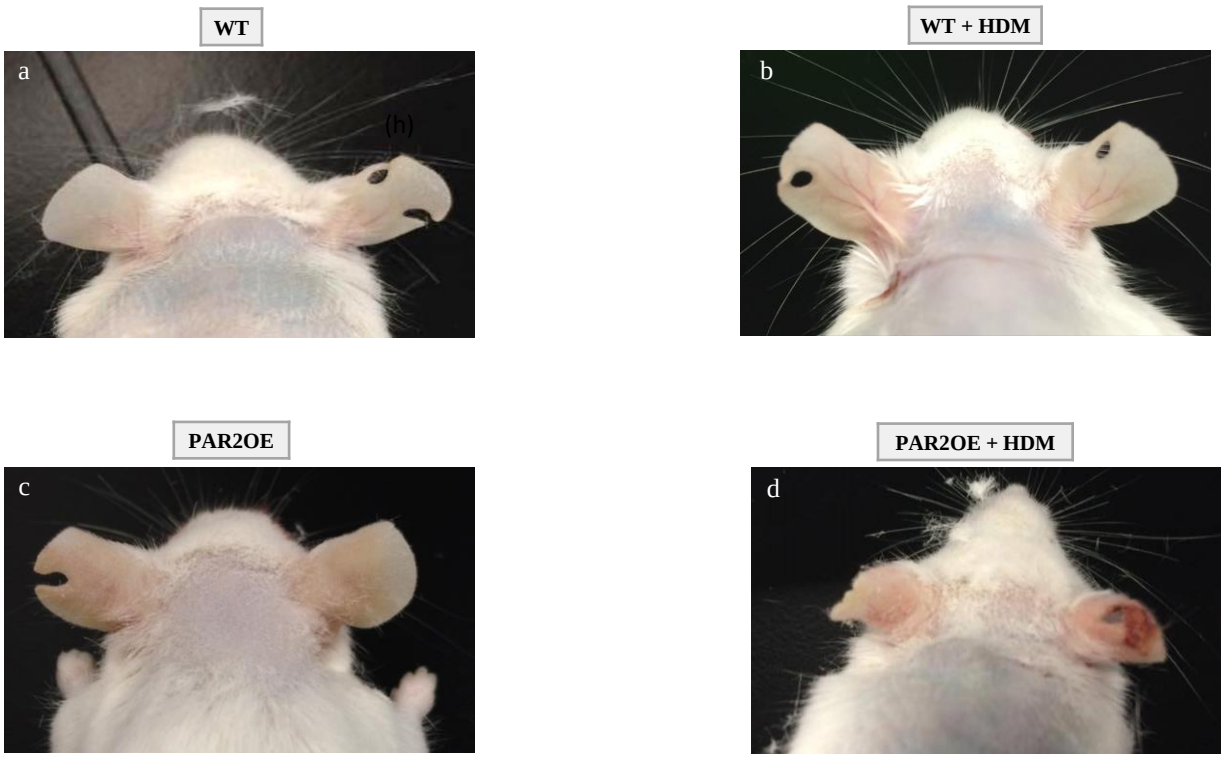
WT
a
(h)
WT + HDM
b
PAR2OE
c
PAR2OE + HDM
d

B

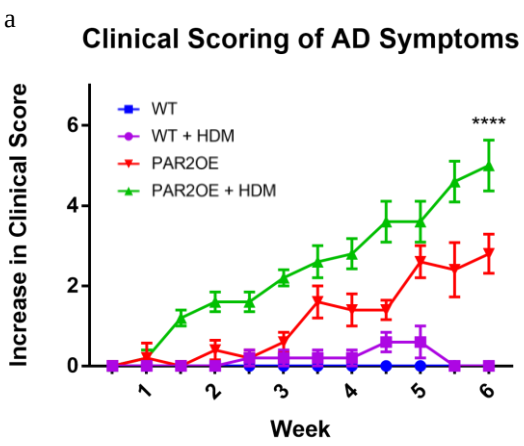
a
Clinical Scoring of AD Symptoms
Increase in Clinical Score
Week
WT
WT + HDM
PAR2OE
PAR2OE + HDM
****

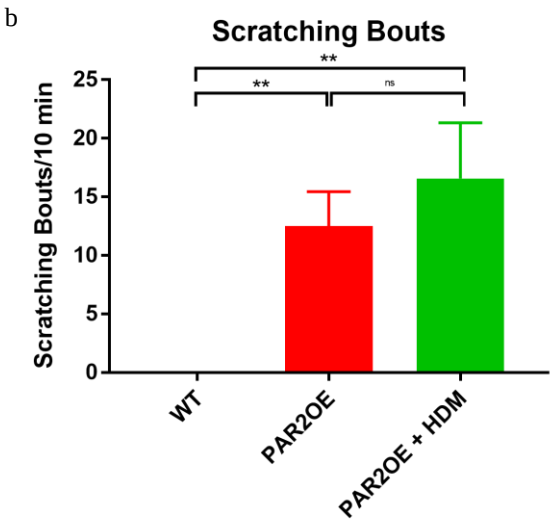
b
Scratching Bouts
Scratching Bouts/10 min
WT
PAR2OE
PAR2OE + HDM
**
ns

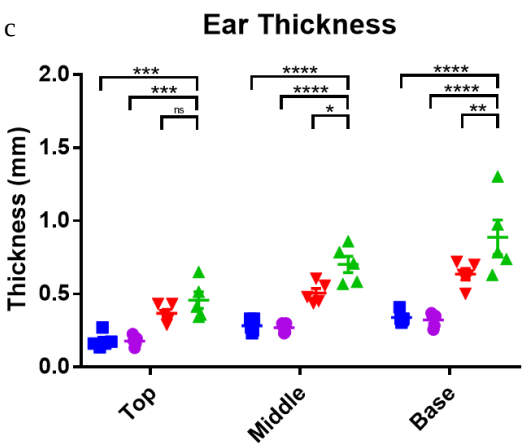
c
Ear Thickness
Thickness (mm)
Top
Middle
Base

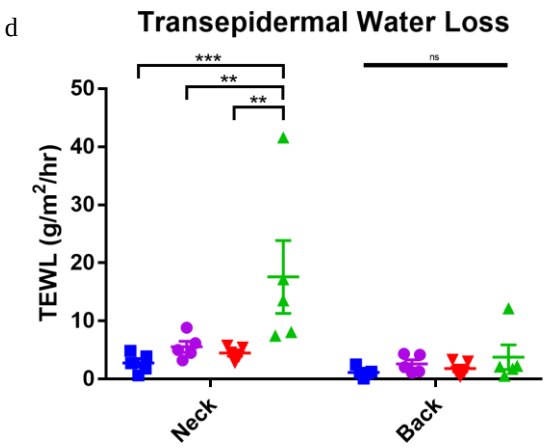
d
Transepidermal Water Loss
TEWL (g/m2/hr)
Neck
Back
ns

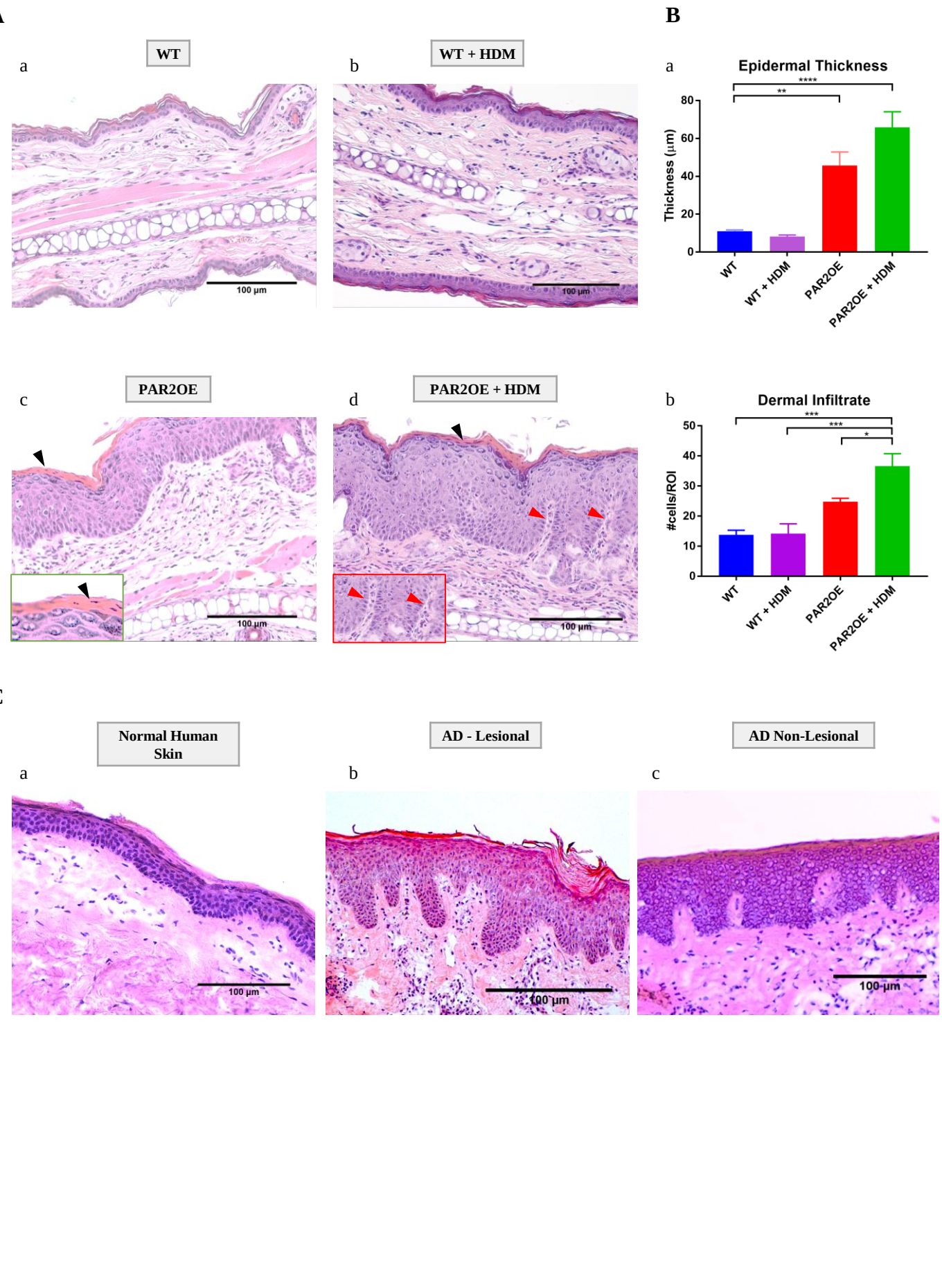
A
WT
a
WT + HDM
b
100 µm
100 µm
PAR2OE
c
PAR2OE + HDM
d
100 µm
100 µm
B
a
Epidermal Thickness
****
**
Thickness (µm)
80
60
40
20
0
WT
WT + HDM
PAR2OE
PAR2OE + HDM
b
Dermal Infiltrate
***
***
*
#cells/ROI
50
40
30
20
10
0
WT
WT + HDM
PAR2OE
PAR2OE + HDM
C
Normal Human Skin
a
AD - Lesional
b
AD Non-Lesional
c
100 µm
100 µm
100 µm

A

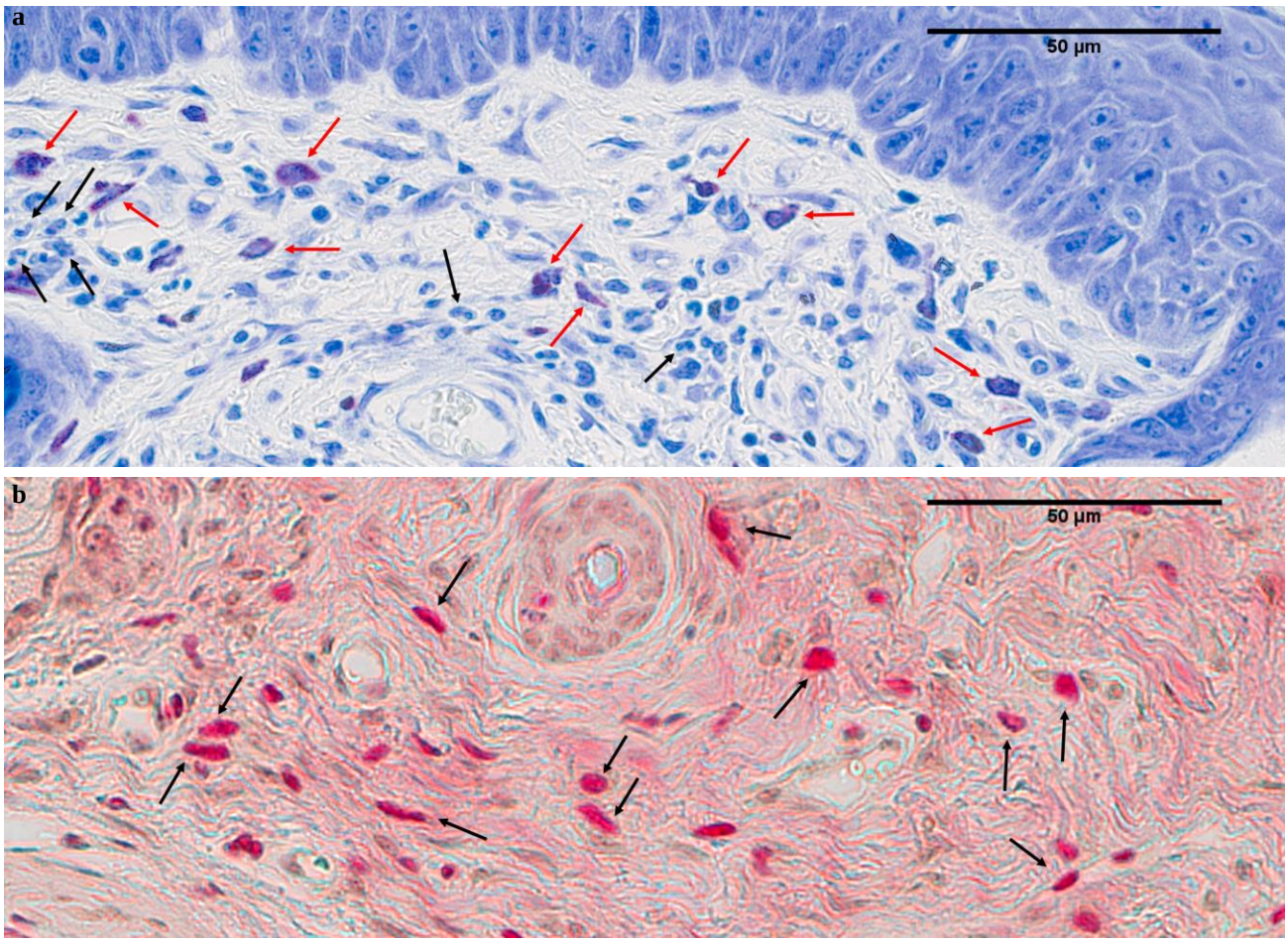
a
50 µm
b
50 µm

B

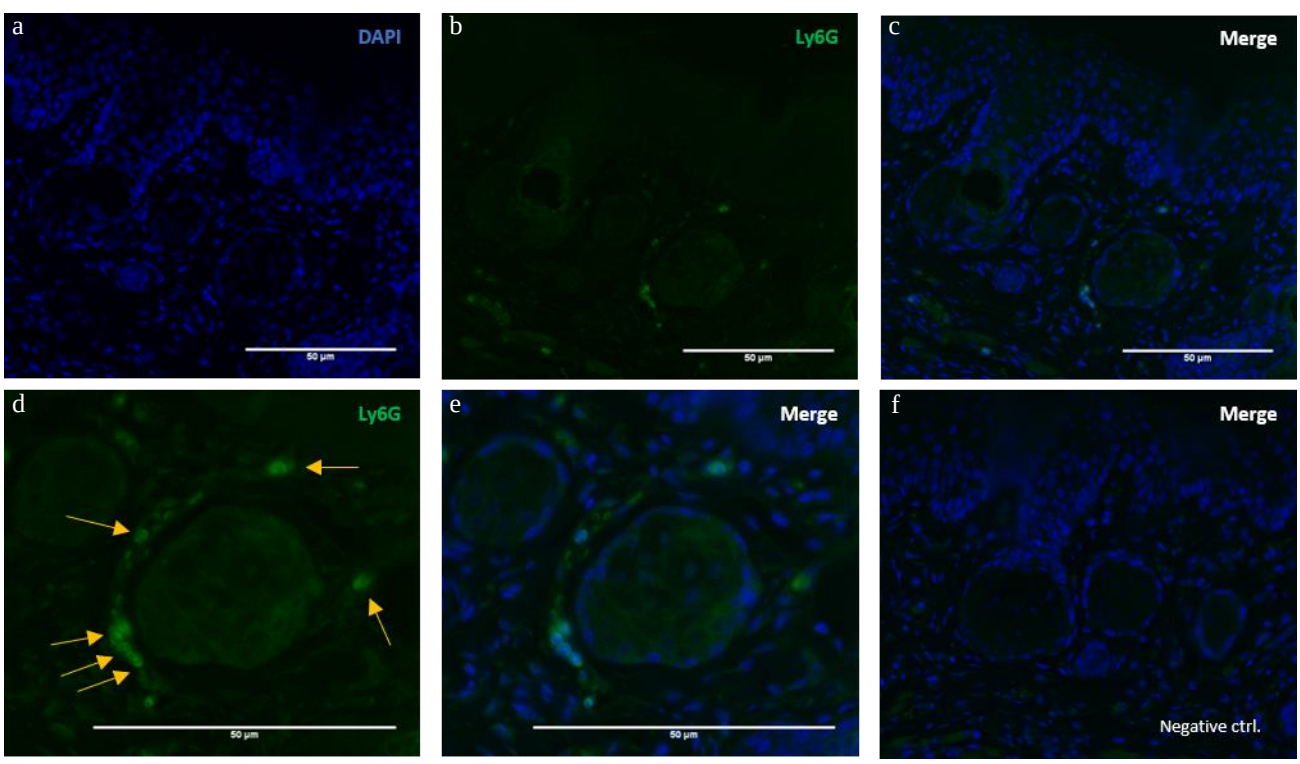
a
DAPI
b
Ly6G
c
Merge
d
Ly6G
e
Merge
f
Merge
Negative ctrl.

C

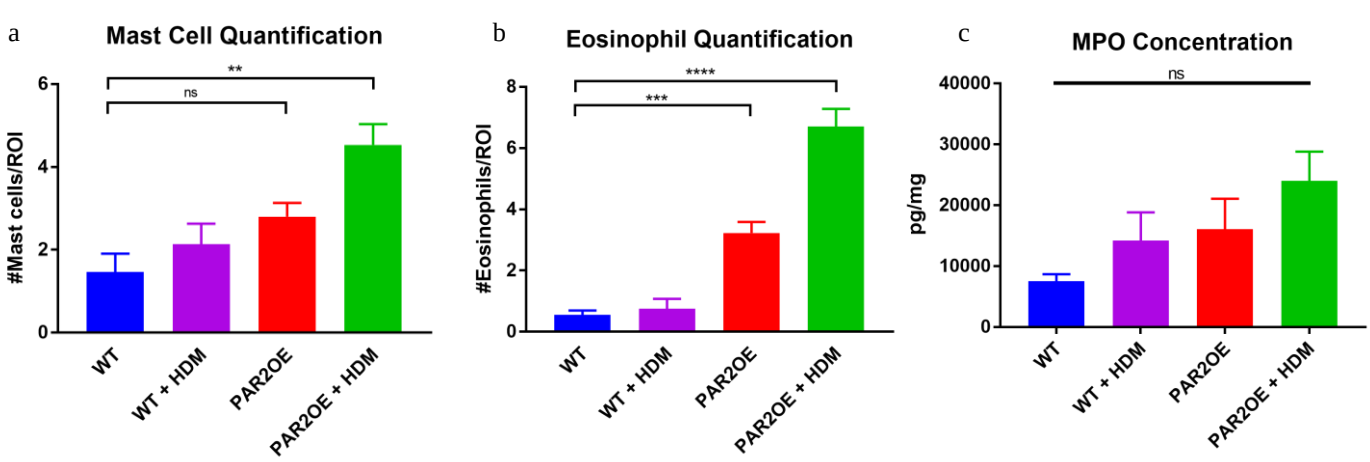
a
Mast Cell Quantification
#Mast cells/ROI
**
ns
WT
WT + HDM
PAR2OE
PAR2OE + HDM
b
Eosinophil Quantification
#Eosinophils/ROI
****
***
c
MPO Concentration
pg/mg
ns

A

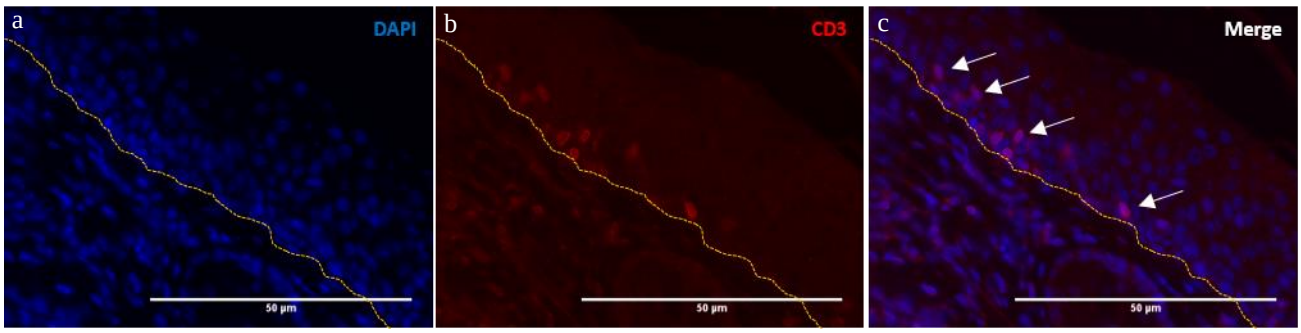
a
DAPI
b
CD3
c
Merge
50 µm
50 µm
50 µm

B

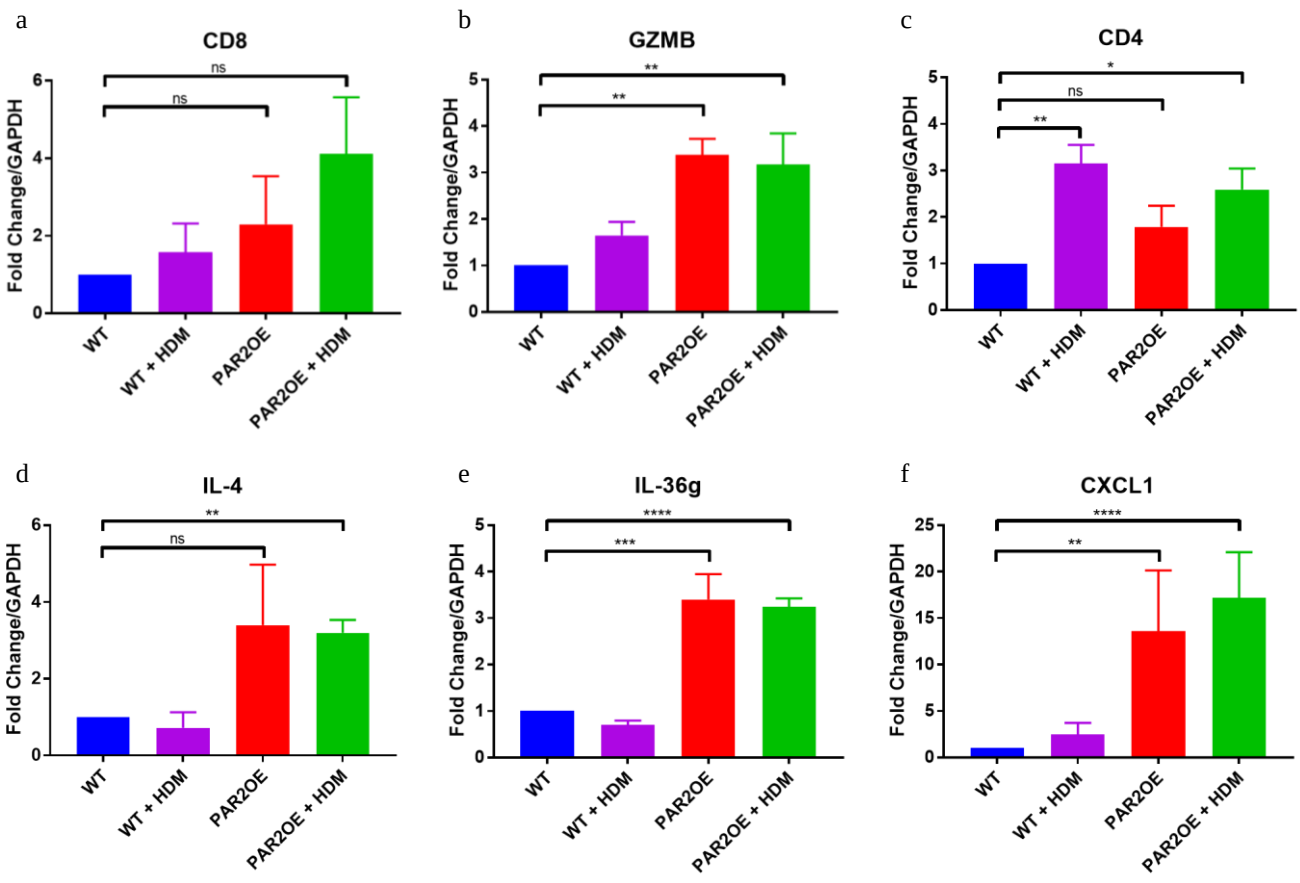
a
CD8
ns
ns
b
GZMB
**
**
c
CD4
*
ns
**
d
IL-4
**
ns
e
IL-36g
****
***
f
CXCL1
****
**
Fold Change/GAPDH
WT
WT + HDM
PAR2OE
PAR2OE + HDM

Supplementary Table 1: Primers used for Genotyping

Strain	Oligo Name	Sequence 5' to 3'
PAR2OE	mGrhP2 for	CAC CCC CTC AGC TAA GAA GGA A
	mGrhP2 rev	CCC TTT GGC AAG AGG AGA GAA A
	mGrhP2 KO	CTG GGT TTC CAA TCT GCC AAT AAG

Supplementary Table 2: Primers used for RT-qPCR

Gene	TaqMan Assay ID
IL-4	Mm00445259_m1
IL-36γ	Mm00463327_m1
CXCL1	Mm04207460_m1
GZMB	Mm00442837_m1
CD4	Mm00442754_m1
CD8	Mm00442837_m1
IVL	Mm00515219_s1
LOR	Mm01962650_s1
FLG	Mm01716522_m1
GAPDH	Mm99999915_g1

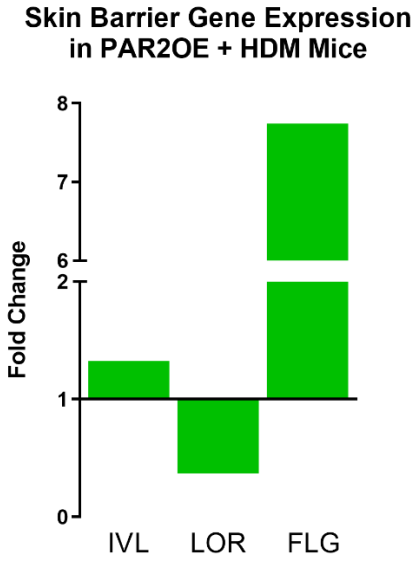

SUPPLEMENTARY FIG 1. Expression of Skin-Barrier Genes in WT and PAR2OE + HDM Mice. Expression of IVL, LOR and FLG genes in ear skin extracts of WT and PAR2OE + HDM mice. Results shown are the average fold change of the PAR2OE + HDM mice in comparison with WT controls. N=3 for IVL, N=6 for LOR and FLG.